

Supplementary materials

Ultrahigh SERS Activity of TiO₂@Ag Nanostructure Leveraged for Accurately Detecting CTCs in Peripheral Blood

Yanping Xu,^{a,b,c†} Dinghu Zhang,^{c†} Jie Lin,^{b,d*} Xiaoxia Wu,^{b,c} Xiawei Xu,^{b,d} Ozioma
Udochukwu Akakuru,^{b,d} Hao Zhang,^{b,d} Zhewei Zhang,^c Yujiao Xie,^{b,d} Aiguo Wu^{b,d*} &
Guoliang Shao^{c*}

^a Second clinical college, Zhejiang Chinese Medical University, Hang Zhou 310053, China.

^b Cixi Institute of Biomedical Engineering, International Cooperation Base of Biomedical Materials Technology and Application, Chinese Academy of Science (CAS) Key Laboratory of Magnetic Materials and Devices & Zhejiang Engineering Research Center for Biomedical Materials, Ningbo Institute of Materials Technology and Engineering, CAS, 1219 ZhongGuan West Road, Ningbo 315201, China.

^c Department of Interventional Radiology, The Cancer Hospital of the University of Chinese Academy of Sciences (Zhejiang Cancer Hospital), Institute of Basic Medicine and Cancer (IBMC), Chinese Academy of Sciences, Hangzhou 310022, China.

^d Advanced Energy Science and Technology Guangdong Laboratory, Huizhou 516000, P.R. China.

*Corresponding authors.

Email addresses:

linjie@nimte.ac.cn (Jie Lin)
aiguo@nimte.ac.cn (Aiguo Wu)
shaogl@zjcc.org.cn (Guoliang Shao)

† Y. Xu and D. Zhang contributed equally to this work.

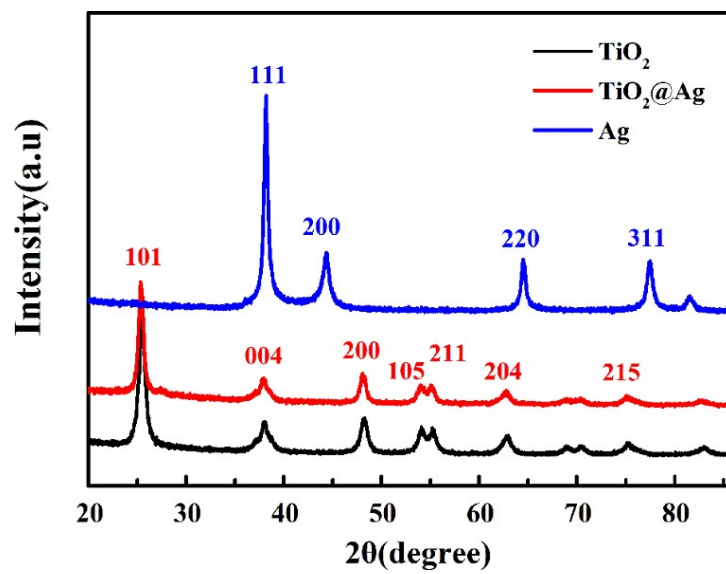


Fig. S1 X-ray diffraction (XRD) spectra of TiO₂, TiO₂@Ag, and Ag.

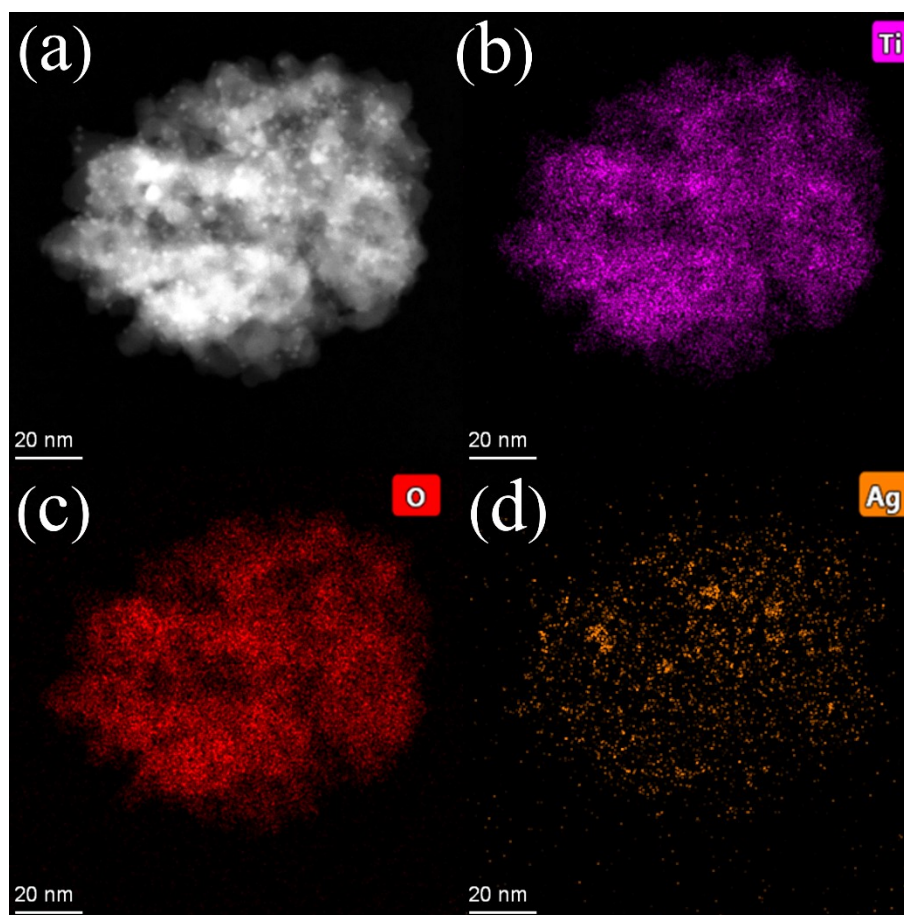


Fig. S2 Element distributions mapping images of Ti, O, and Ag in $\text{TiO}_2@Ag$ nanostructures.

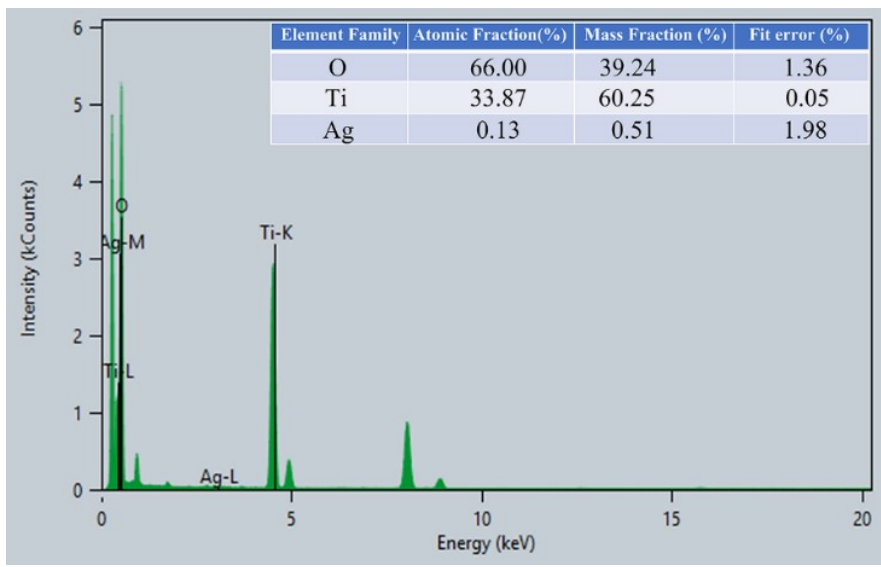


Fig. S3 Energy-dispersive spectroscopy (EDS) characterization of TiO₂@Ag.

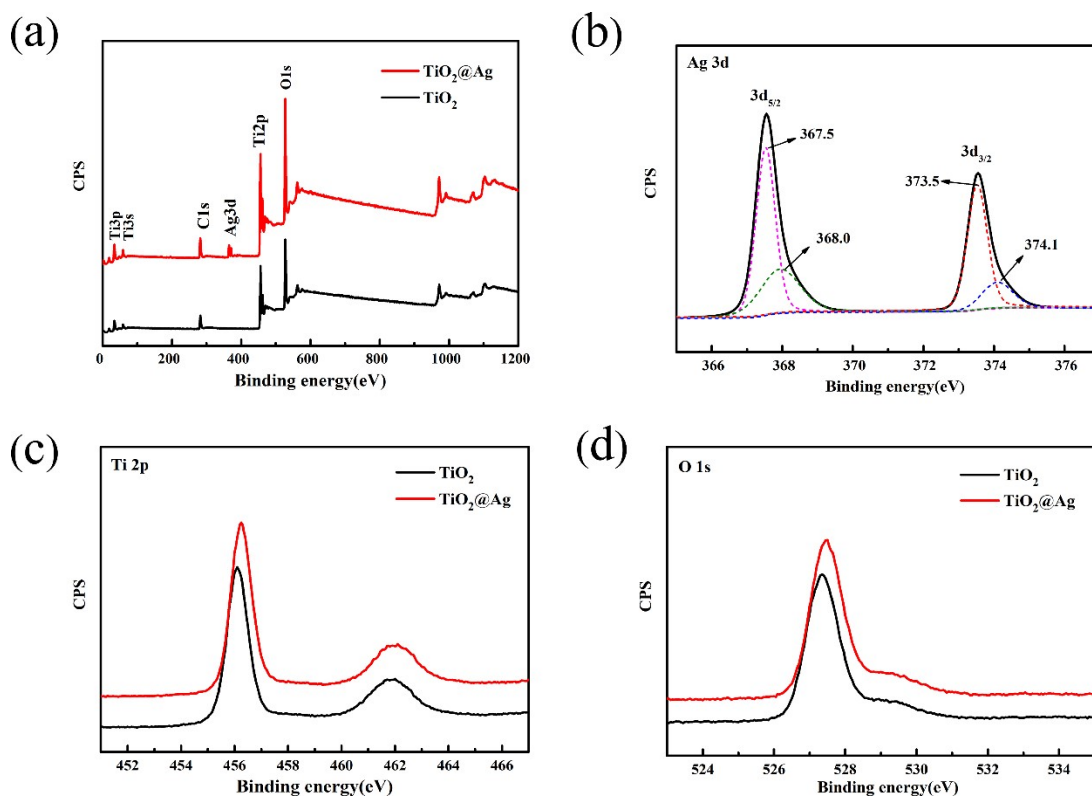


Fig. S4 XPS spectra of survey spectrum (a), Ag 3d (b), Ti 2p (c), and O 1s (d) of TiO_2 and $\text{TiO}_2@Ag$ samples, respectively.

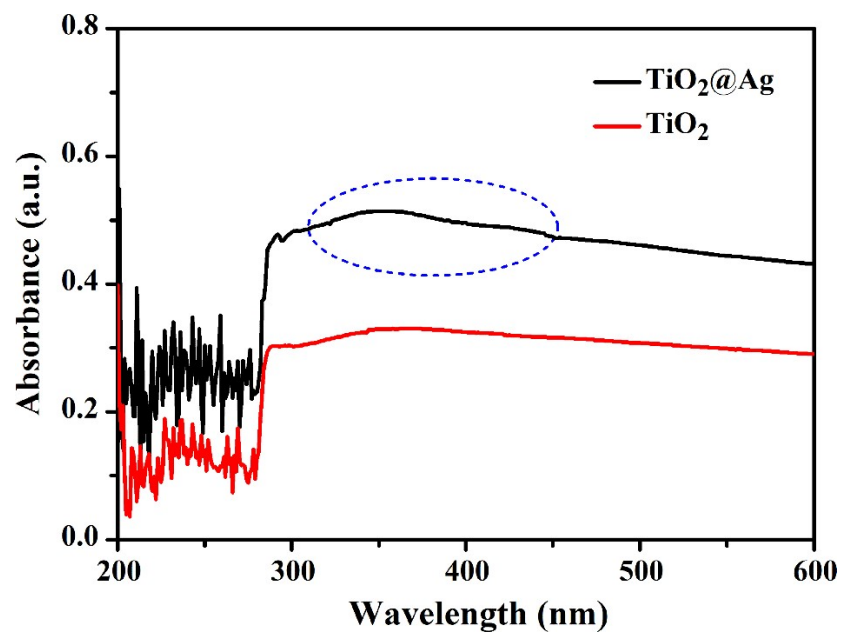


Fig. S5 UV-vis spectroscopy of $\text{TiO}_2@Ag$, and TiO_2 .

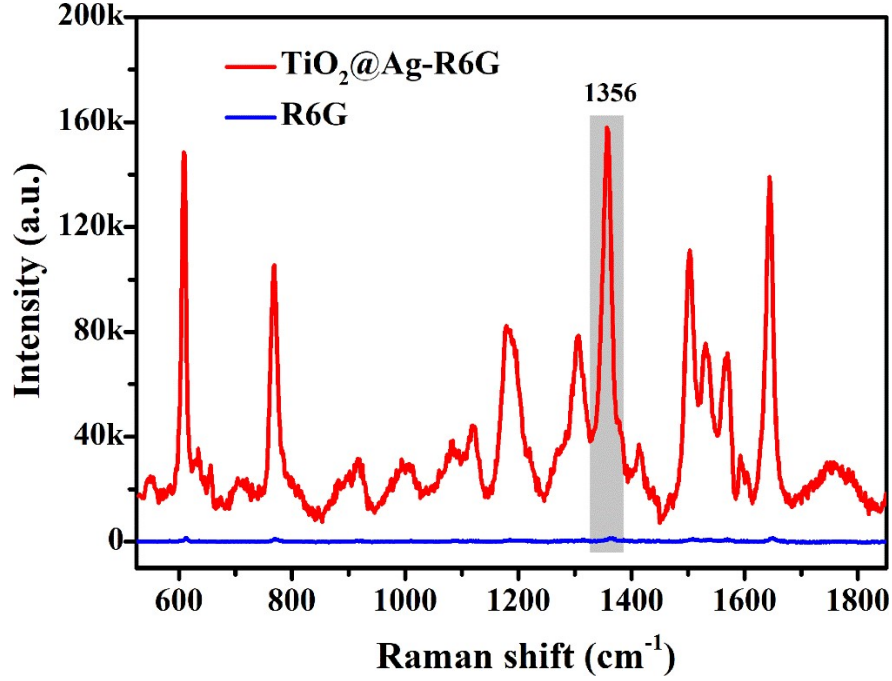


Fig. S6 Raman spectra of R6G molecule (5×10^{-5} M) adsorbed on $\text{TiO}_2@Ag$ NPs and pure SERS signal of R6G molecules (5×10^{-2} M).

Enhancement factor (EF) calculation of $\text{TiO}_2@Ag$ NPs was based on equation (1):

$$EF = (I_{\text{SERS}} / N_{\text{ads}}) / (I_{\text{bulk}} / N_{\text{bulk}}) \quad (1)$$

Where N_{ads} and N_{bulk} imply the number of R6G molecules adsorbed on the $\text{TiO}_2@Ag$ NPs substrate and R6G molecules in normal Raman substrate, respectively. I_{SERS} and I_{bulk} are the vibration peak (1356 cm^{-1}) intensity of R6G molecules on $\text{TiO}_2@Ag$ NPs substrate, and normal Raman spectrum of R6G molecules, respectively.

During the SERS experiment, 100 μL of ethanol aqueous R6G solution (5×10^{-2} M) was dried onto $0.4 \text{ cm} \times 0.4 \text{ cm}^2$ silicon wafer. N_{Raman} was lied on equation (2).

$$N_{\text{bulk}} = 100 \mu\text{L} \times 5 \times 10^{-2} \text{ mol/L} \times 8 \times 6.02 \times 10^{23} \text{ mol}^{-1} \times 1.3 \mu\text{m}^2 / 0.16 \text{ cm}^{-2} \quad (2)$$

where d is the diameter of the light spot estimated as $d = 1.22 \lambda/\text{NA}$, λ is incident wavelength 532 nm, the numerical aperture of the objective lens $N_A = 0.5$, the laser spot is $\sim 1.3 \mu\text{m}^2$. On the basis of equation (2), N_{bulk} was estimated as $\sim 1.95 \times 10^{12}$.

In addition, N_{ads} is synergistically determined by laser spot illuminating the $\text{TiO}_2@\text{Ag}$ -R6G substrate, and the density of R6G molecules, N_{ads} is concluded as:

$$N_{\text{ads}} = \sigma \times 1.3 \mu\text{m}^2 \times 6.02 \times 10^{23} \text{ mol}^{-1} \quad (3)$$

Where σ is the density of R6G molecule absorbed onto $\text{TiO}_2@\text{Ag}$ substrate, which is approximated to $\sim 0.5 \text{ nM cm}^{-2}$ (3). N_{ads} is concluded as $\sim 3.91 \times 10^6$. I_{SERS} is the Raman peak intensity at 1356 cm^{-1} of R6G molecules on $\text{TiO}_2@\text{Ag}$ NPs, while I_{bulk} represents the Raman peak intensity at 1356 cm^{-1} of pure R6G molecule (fig S6). $I_{\text{SERS}} = \sim 135065$ and $I_{\text{bulk}} = \sim 882$. Substituting these values into equation (1), EF of $\text{TiO}_2@\text{Ag}$ NPs was concluded to be $\sim 7.61 \times 10^7$.

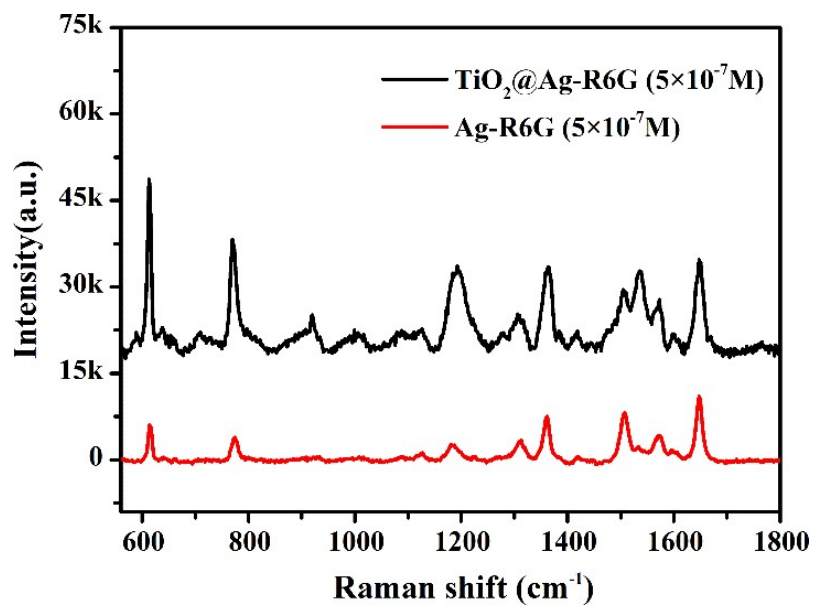


Fig. S7 SERS signal of R6G ($5 \times 10^{-7} \text{ M}$) molecule adsorbed on $\text{TiO}_2@Ag$ nanostructure, and Ag NPs.

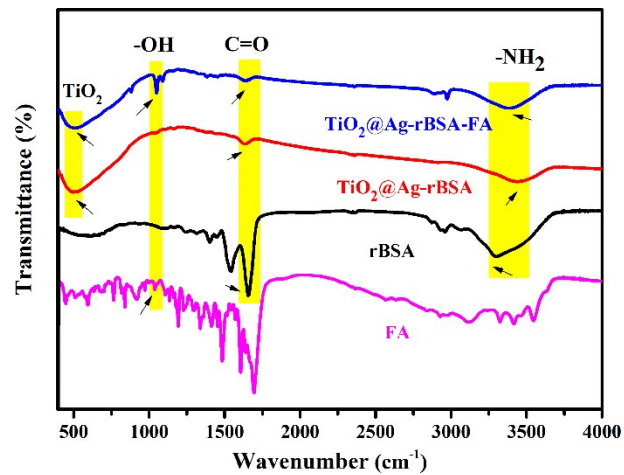


Fig. S8 FT-IR spectra of FA, rBSA, TiO₂@Ag-rBSA, and TiO₂@Ag-rBSA-FA.

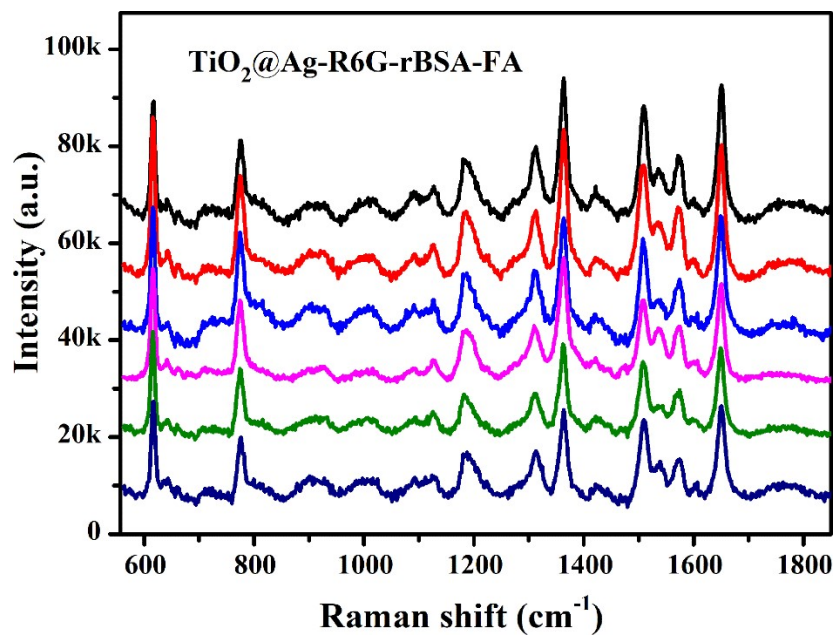


Fig. S9 SERS spectra of R6G (5×10^{-3} M) molecule collected from six TiO₂@Ag-rBSA-FA SERS bioprobes; Excitation wavelength: 532 nm; Laser power: 0.1 mW; Lens: 50× objective; Accumulations: 10 s.

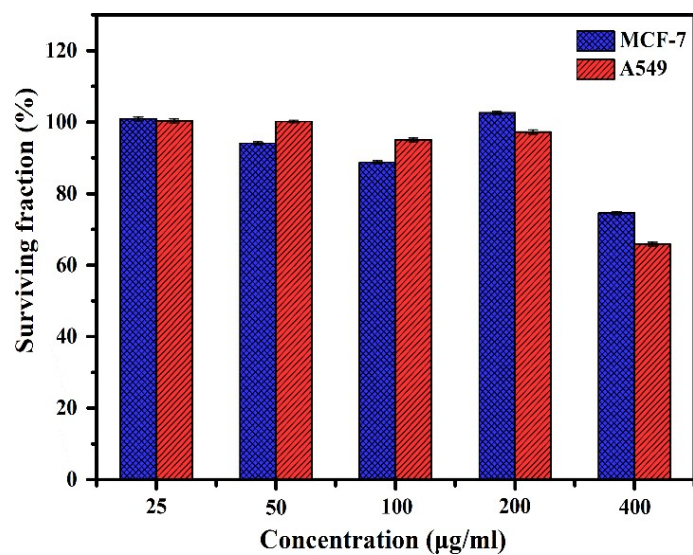


Fig. S10 Cell viability of A549 and MCF-7 cells co-incubated with $\text{TiO}_2@\text{Ag-R6G-rBSA-FA}$ bioprobe for 24 h with different $\text{TiO}_2@\text{Ag}$ concentrations.

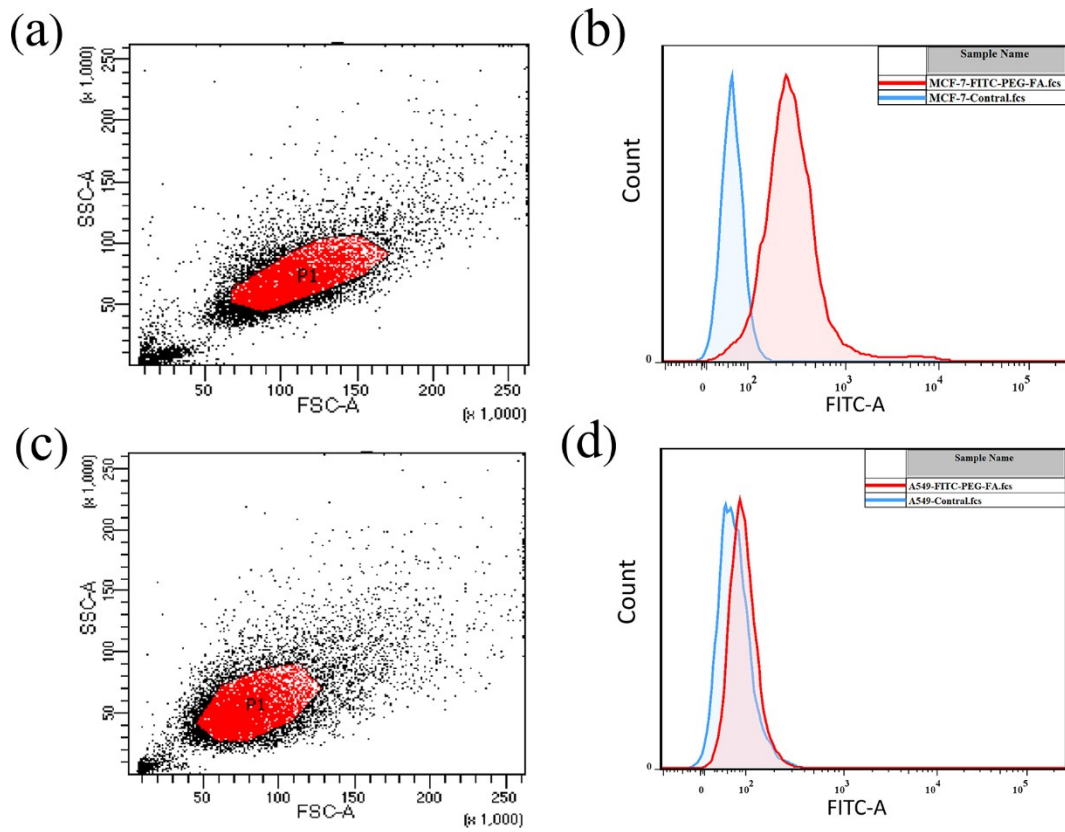


Fig. S11 FCS analysis of MCF-7 and A549 cells incubated with 20 μ L FA-PEG-FITC (red) and PBS (blue).

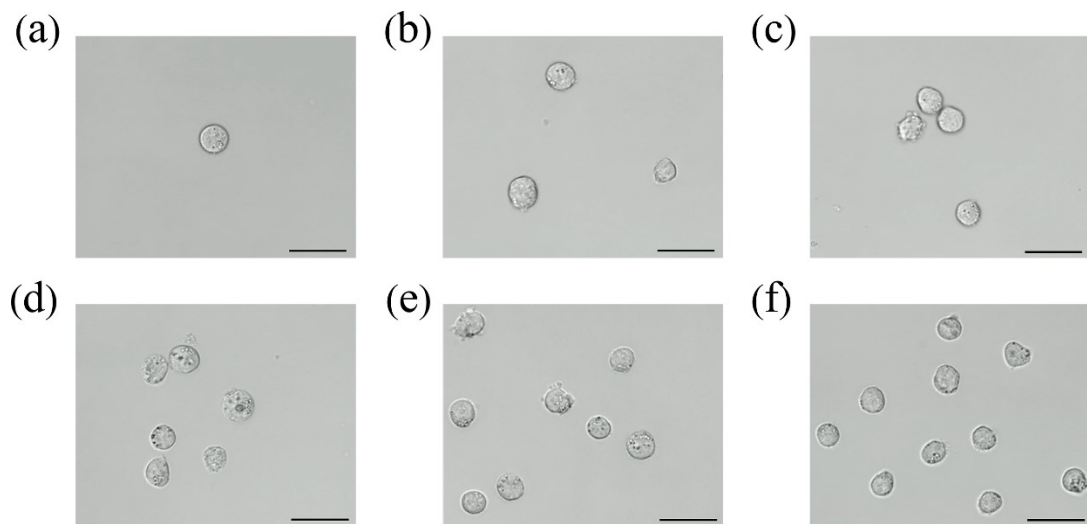


Fig. S12 HeLa cell count of bright field under laser scanning confocal microscope.

Scale bar: 25 μm .

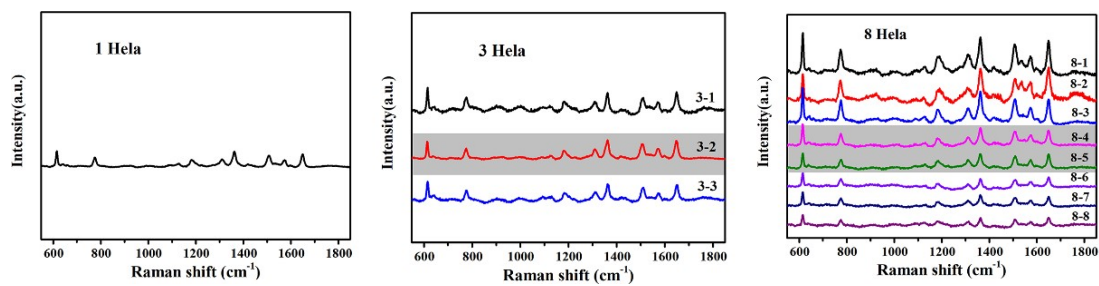


Fig. S13 Detection sensitivity of the TiO₂@Ag-R6G-rBSA-FA SERS bioprobe for different numbers of HeLa cells in the rabbit blood.

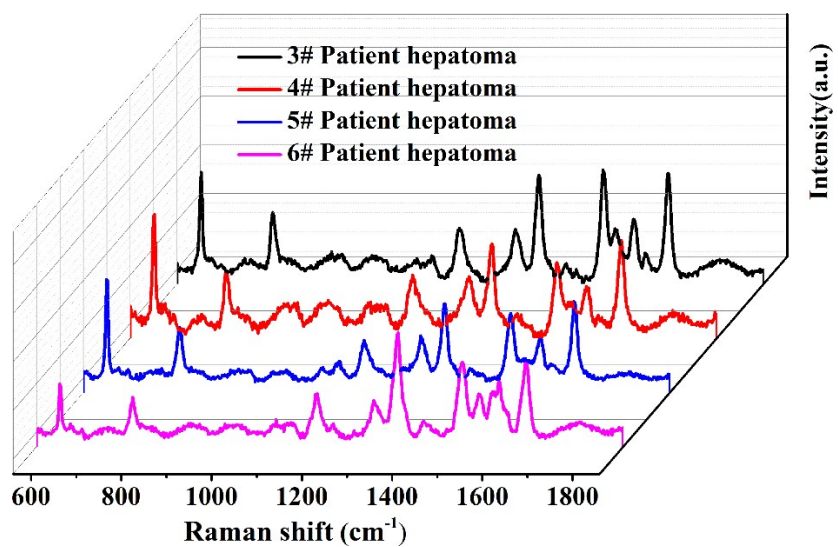


Fig. S14 $\text{TiO}_2@\text{Ag-R6G-rBSA-FA}$ SERS bioprobe was utilized for CTCs detection in peripheral blood of four liver cancer patients.